iJRASET
International Journal For Research in Applied Science and Engineering Technology

INTERNATIONAL JOURNAL FOR RESEARCH

IN APPLIED SCIENCE & ENGINEERING TECHNOLOGY

Volume: 9 **Issue:** XI **Month of publication:** November 2021

DOI: https://doi.org/10.22214/ijraset.2021.38671

www.ijraset.com

Call: 08813907089 | E-mail ID: ijraset@gmail.com

International Journal for Research in Applied Science & Engineering Technology (IJRASET)
ISSN: 2321-9653; IC Value: 45.98; SJ Impact Factor: 7.429
Volume 9 Issue XI Nov 2021- Available at www.ijraset.com

Static Analysis of Wheel Rim Using Inventor Software

Valentin Mereuta
Faculty of Engineering, University "Dunarea de Jos", Galati, Romania

Abstract: ***In this paper the 3D model of the real wheel rim was designed using Autodesk Inventor and finite element analysis is performed using Nastran software by applying restrictions and loads conditions. The materials taken for static analysis are steel, aluminum alloy, magnesium alloy and titanium alloy. Following the comparative study for the four models, it can be specified that the importance of the material for the construction of the rims depends on the mass properties and their design.***
Keywords: Wheel Rim, Static analysis, Autodesk Inventor Nastran

I. INTRODUCTION

The study of finite element analysis can give information on the rim parameters: size, weight, design and materials. The dimensions of the rim provide information on the space between the rim and the brake rotor. If the diameter of the wheel rim is larger, there will be a greater possibility of air circulation around the brakes and, therefore, an efficient cooling is obtained. The weight of the rim is also an important parameter and light vehicles are easier to handle. Another important factor in handling vehicles is related to the strength of the wheel and its flexibility. A stiffer wheel will reduce wheel flexibility. When performing an analysis of the state of stresses and strains, it is important to accurately apply the limit conditions, constraints and loads. For wheels equipped with pneumatic tires, it is not obvious what these loading conditions are [1]. The forces act on the wheel rim due to both the air pressure in the tire and the reaction of the tread on the tire. The way these forces are transmitted through the tire to the rim has a significant impact on the state of tension in the wheel. Although modeling of the tire is also possible, it is generally useless when studying the state of tension in the wheel, leading to an increase in the complexity of the model. However, there are established analytical and empirical ways to simplify the influence of the tire in terms of setting limit conditions, which can be applied directly to the rim [2].
The complexity of modeling the tire-rim interaction and finite element analysis is given primarily by the toroidal shape of the tire that comes into contact with the flat surface of the tread, which leads to a deformation of it, a deformation that must be large enough to form a plane contact, requiring nonlinear modeling. Second, a tire is not made of a homogeneous isotropic solid material, but is a composite structure with a rubber matrix surrounding anisotropic textile casings and bead wires.
Their modeling would require considerable solution and processing time and a fairly high-performance calculation system is required, the interactions between the tire and the tread being presented in the specialized works [2, 3].
The forces act on the rim due to two primary sources: the air pressure inside the tire and the reactions on the tread. The air inside the tire exerts a uniform pressure on all the inner sides of the tire and rim; this is the distension pressure, P. If the pressure acts on the inside of the tread, it is contained by the carcass and bead of the tire, causing internal tensions in the tire, but there are no reaction forces on the rim. However, if the distension pressure acts on the sidewall of the tire, it causes the bead ring to twist outwards. These lateral forces, Fs, are given by the rim flange.

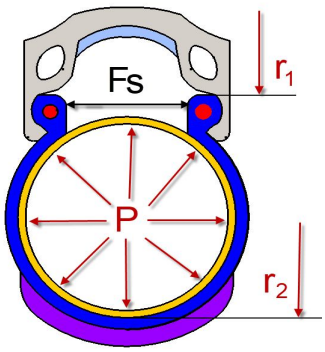

Fig. 1 Pressure distribution inside the tire

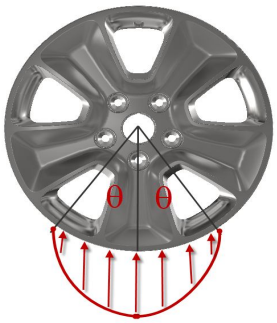

Fig. 2 Forces distribution on the rim

Calculating the force on the side wall of the rim flange involves integrating the pressure over the tire area. The integration is quite simple, because it only affects the area of the side wall projected on the vertical plane. This area is given by the equation:

$$A = \pi \cdot \left(r_2^2 - r_1^2\right) \tag{1}$$

The surface is multiplied by the pressure P to give the total force acting on each side wall of the tire. The force acting on the rim flange is half of it, because the lower part of the sidewall is constrained by the rim, while the upper part of the sidewall is constrained by the tread of the tire. Therefore, these forces are given by the equation:

$$F_s = \frac{1}{2} \cdot P \cdot \pi \cdot \left(r_2^2 - r_1^2\right) \tag{2}$$

The other forces acting on the rim result from the reaction forces of the tread. These can be classified as vertical forces supporting the weight of the vehicle, torque resulting from acceleration and braking forces and axial forces occurring when cornering. These forces are transferred through the bead and the flange of the rim, but are not constant over the entire circumference of the rim. Instead, these forces act on a section of the rim, related to the contact pitch of the tires and stiffness and given by the loading angle, θ. The forces are cosinusoidally distributed over this region, Fig. 2.

The loading angle depends on the combination of the tire and the rim, the tire pressure and the reaction force on the tread. In practice, it is not possible to determine this analytical angle and an empirical method must be used. One option is to run the simulation with several different loading angles and observe how they influence the wheel stresses, then use a certain angle, the results can be compared with experimental measurements in order to determine the actual angle of loading [4].

Due to the rotation of the wheel and the periodic nature of the spokes, the wheel stresses will be between two extreme values. In one state, the vertical reaction to the running track will be directly centered towards the spoke and in the other it will fall halfway between the spokes.

For each wheel rotation, each spoke will perform a cycle that should be considered for fatigue calculations. Additional reaction forces of the running track also occur when turning, braking or accelerating.

Turns result in an axial force that is transferred through the flange, which can have a sinusoidal distribution and act over a loading angle similar to the vertical reaction force.

In conclusion, it can be stated that there are five forces acting on the rim:

1) Distension pressure, P, acting uniformly on the inner faces of the rim which does not come into contact with the tire.
2) The reaction of the pressure on the side wall, F_S, acting on both flanges of the rim.
3) The vertical reaction to the running track, F_V, distributed sinusoidally on both heels.
4) Axial steering reaction, F_A, sinusoidally distributed over one of the rim flanges depending on the steering direction.
5) The tangential braking or turning reaction, F_T, which acts on the same region of the bead seats as the vertical reaction to the running track which is also sinusoidally distributed, with the tangential load transfer in correlation with the normal force.

Rahul K. Jape [5] designed an aluminum alloy wheel in order to optimize its mass, by finite element analysis using Catia software.
Rakesh B.
Thakare [6] studied the FEM analysis of the aluminum wheel under different loads to determine the exact place of cracks initiation leading to rim failure, using Ansys software.

Meghashyam et al. [7] described the static analysis of rim using ANSYS software for two different materials, forged steel and aluminum. In addition to this rim which is subjected to modal analysis (vibration analysis), its performance is analyzed by a dynamic analysis.

II. RIM AND BRAKE DISC DESIGN

Solid modeling of the rim and ventilated brake disk was done using Autodesk Inventor version 2021 with the literature data.

The solid models of the discs and the rim are shown in Fig. 3.

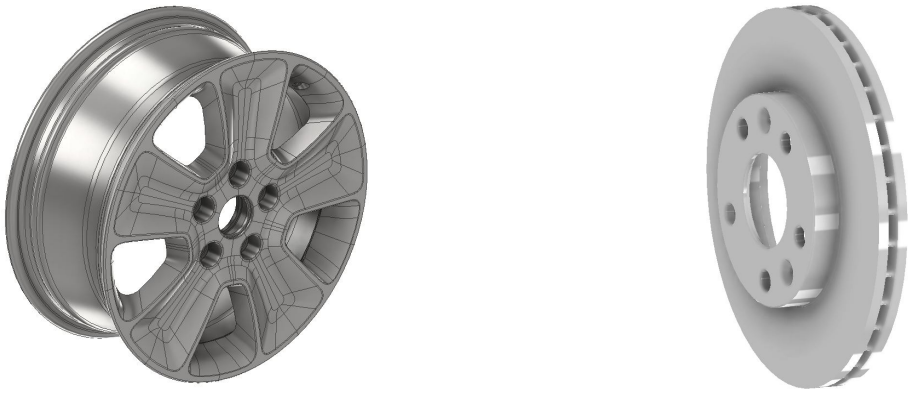

Fig. 3 A geometrical model of the rim and ventilated brake discs

III.STATIC ANALYSIS

Finite element analysis was performed with the specific Nastran module included in the Autodesk Inventor software.
In order to obtain the best possible results and at the same time in order to be able to run the simulation with as few system requirements as possible, only the subassembly consisting of the rim and the wheel hub was maintained. The static analysis is chosen as the type of analysis.

A. Choosing Material

In the study presented below, four materials used in the construction of the rims were considered in accordance with the literature [5] – [7]: steel, aluminum alloy, magnesium alloy and titanium alloy, materials with properties shown in Table 1.

TABLE I
material properties

Parameters	Steel	Aluminium 6061	Magnesium	Titanium
Young's Modulus [MPa]	210000	68900	44000	102810
Poisson's Ratio	0.30	0.33	0.35	0.36
Shear Modulus [MPa]	80000	25864	16300	44000
Mass Density [Ns^2/mm^4]	7.85E-09	2.7E-09	1.74 E-09	4.51 E-09
Tensile Strength [MPa]	345	310	180	344.5
Yield Strength [MPa]	207	275	115	275.6
Thermal Expansion Coefficient	1.2E-05	2.36E-05	2.61 E-05	8.6 E-06
Thermal Conductivity N/(sec ^oC)	5.6E+01	1.67 E+02	1.506 E+02	1.644 E+01
Specific Heat $mm^2/(sec^2\ ^oC)$	4.8E+08	8.97 E+08	1.03 E+09	5.23 E+08

B. The Restrictions Condition

Restrictions have been imposed on the brake disc, Fig. 4 and connections were made between the disc and the rim. Autodesk Inventor Nastran offers the possibility of imposing bolt assembly connections, bolt type connector, Fig. 5, specifying the elements between which the assembly is made and the type of assembly.

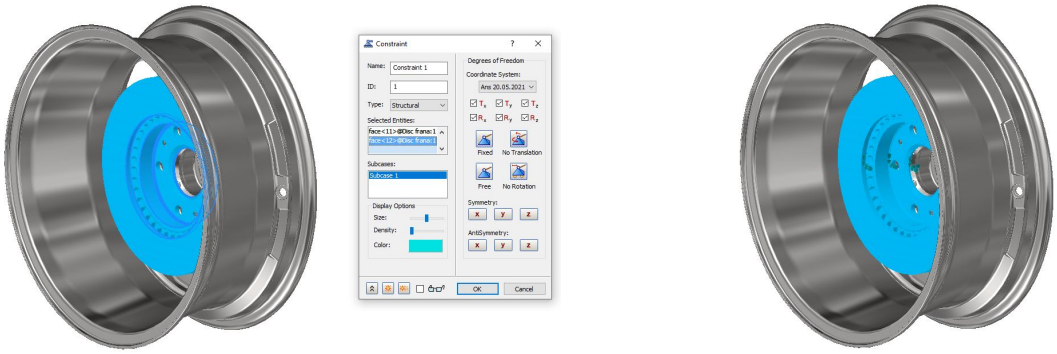

Fig. 4 A restrictions condition

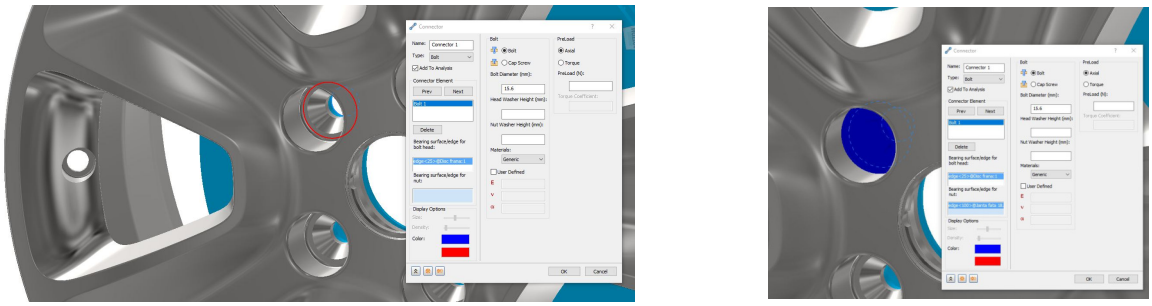

Fig. 5 Conector type bolt

C. Generate Meshing

To generate the mesh, the automatic generation mode was used with parabolic element order, the assembly model of the rim being meshed into 63806 elements and 117795 nodes.

D. Load Conditions

The next step was to apply loads to the rim.

1) *Tire Pressure:* The air pressure applied to the rim, a uniform pressure on the inner sides of the rim which are not in contact with the tire. Since the literature specifies a maximum air pressure in the range of 40 … 50 psi, the most unfavorable value for the rim was adopted, 50 psi, i.e. 0.345 MPa, Fig. 6.

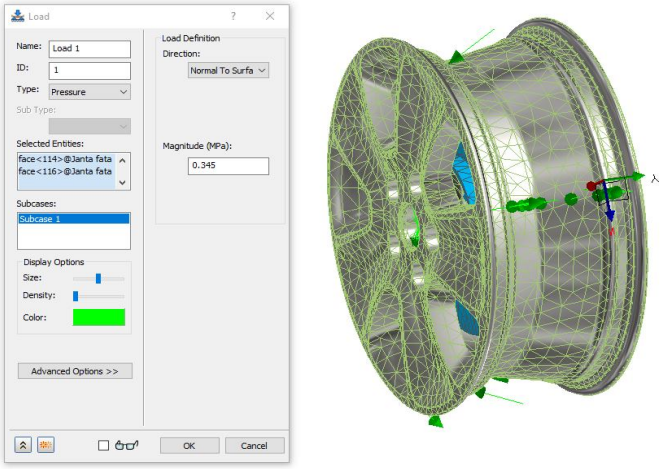

Fig. 6 Tire pressure

2) *The Force Due to the Mass of the Vehicle:* The total mass was required to be evenly distributed on the four wheels. A force value on the wheel, due to the weight of the vehicle, of 4522.41N was obtained. This force was applied to the rim according to Fig. 7.

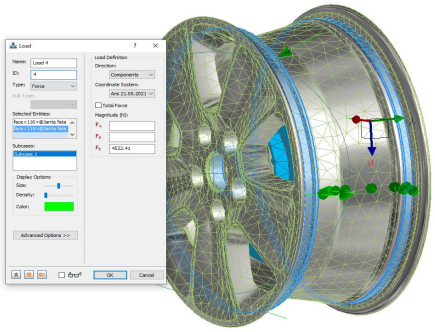

Fig. 7 Force applied to the rim

Force on the sidewall, using the equation for F_S, (Ec. 2.), a reaction force of 24.525 N was obtained, and due to the symmetry of the model, this force is reduced by half and then applied separately, in the normal direction, on each side wall of the rim, Fig. 8.

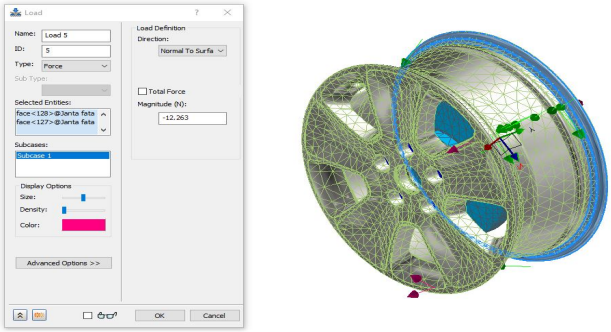

Fig. 8 Force on the sidewall

E. Static Analysis Results

The following figures show the results obtained from the FEM analysis for the steel rim. Low values were obtained both in terms of Von Mises stresses (26.278 MPa), Fig. 9 as well as for the maximum deformations (0.06 mm), Fig. 10.

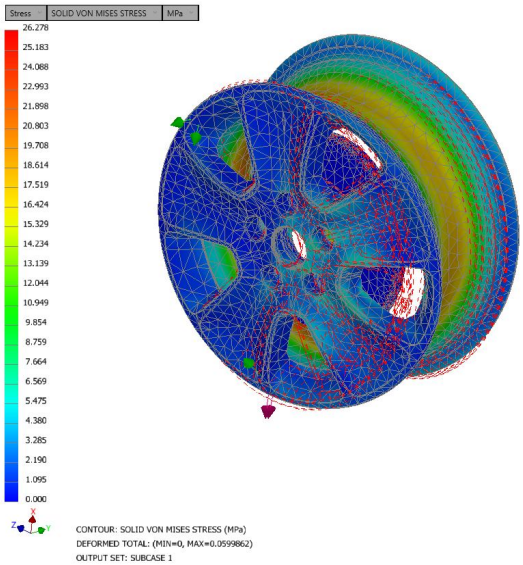

Fig. 9 Von Mises stress – steel rim

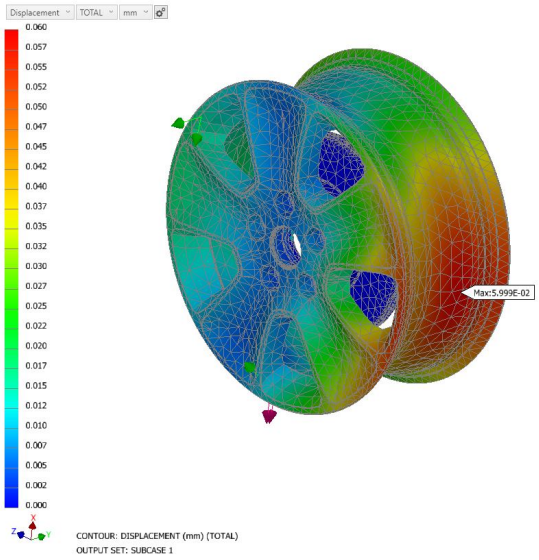

Fig. 20 Total deformation - steel rim

The following figures show the results obtained, following the FEM analysis, for the aluminum alloy rim.
Low values were obtained both in terms of Von Mises stresses (26.662 MPa), Fig. 11 as well as for the maximum deformations (0.132 mm), Fig. 12.

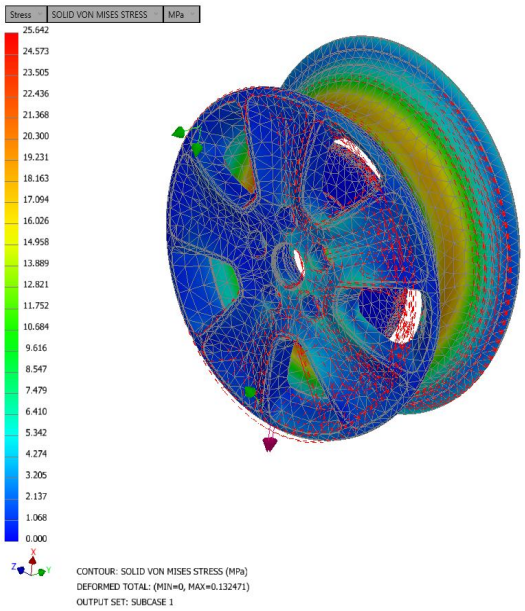

Fig. 31 Von Mises stress – aluminum rim

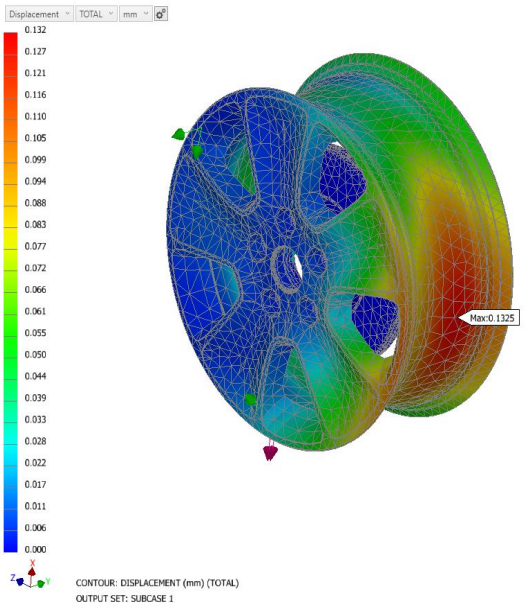

Fig. 42 Total deformation - aluminum rim

The figures 13 and 14 show the results obtained, following the FEM analysis for the magnesium alloy rim.
Low values were obtained for the Von Mises stresses (25.362 MPa) Fig. 13 as well as for the maximum deformations (0.191 mm), Fig. 14.

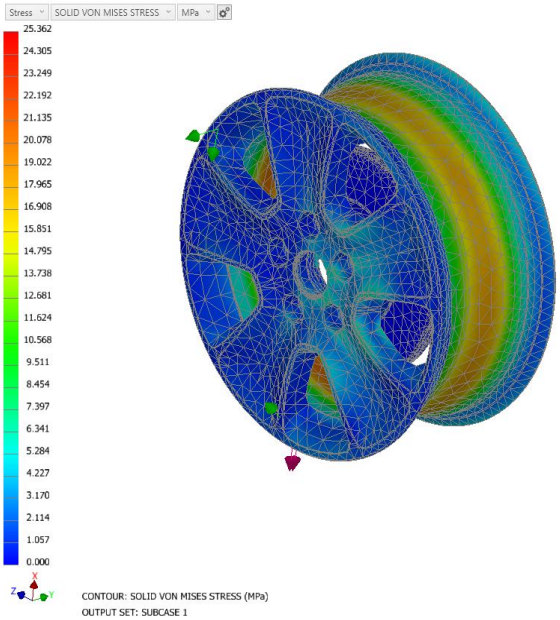

Fig. 53 Von Mises stress – magnesium rim

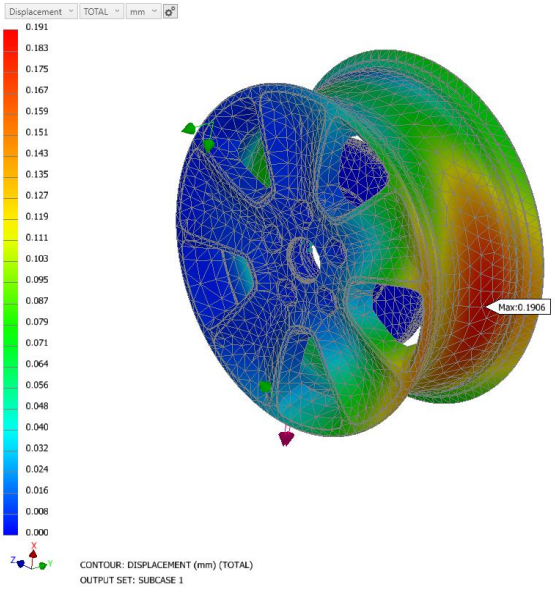

Fig. 64 Total deformation - magnesium rim

Low values were also obtained for the titanium alloy rim, the Von Mises stresses registering a maximum of 25.974 MPa, Fig. 15 and the maximum deformations were 0.090 mm, Fig. 16.

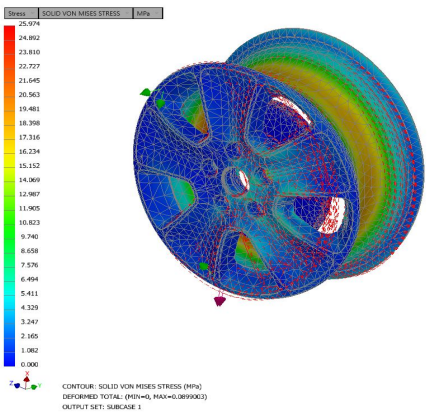

Fig. 75 Von Mises stress – titanium rim

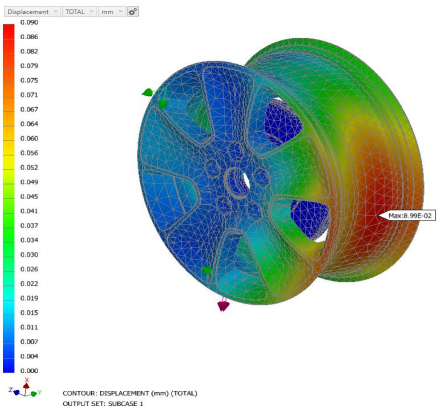

Fig. 86 Total deformation - titanium rim

In the following Fig. 17 - 20 are presented the information related to the general characteristics, mass and inertia for all four rim models analyzed.

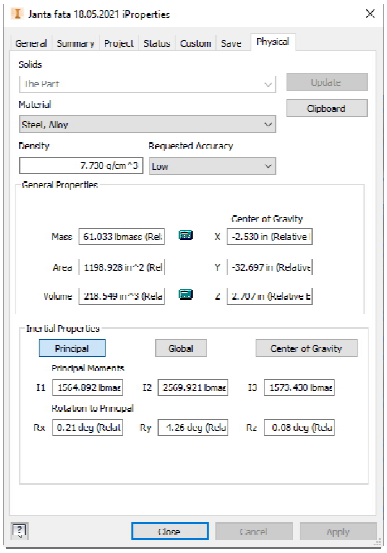

Fig. 97 Physical properties - steel rim

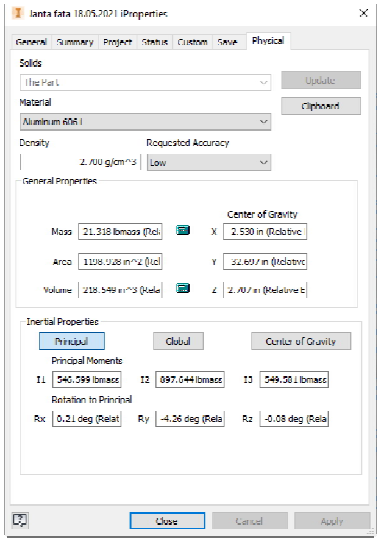

Fig. 108 Physical properties - aluminum rim

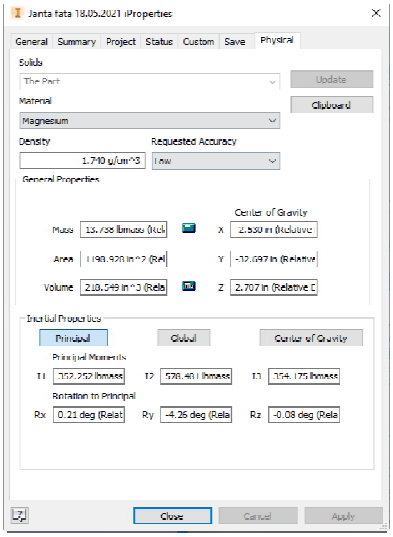

Fig. 119 Physical properties - magnesium rim

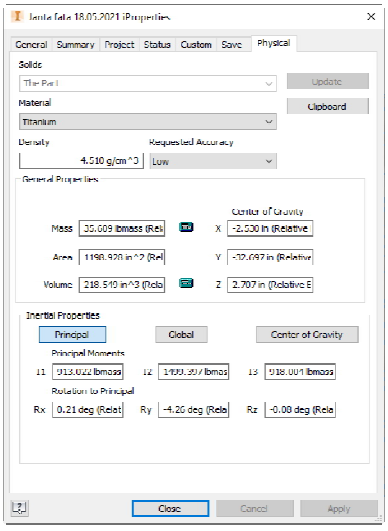

Fig. 20 Physical properties - titanium rim

In order to have a better representation of the obtained results, they have been tabulated and are presented in the form of a graph in Fig. 21.

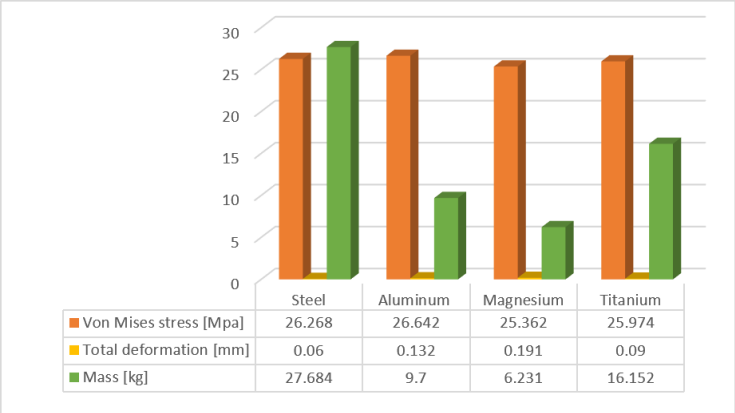

	Steel	Aluminum	Magnesium	Titanium
Von Mises stress [Mpa]	26.268	26.642	25.362	25.974
Total deformation [mm]	0.06	0.132	0.191	0.09
Mass [kg]	27.684	9.7	6.231	16.152

Fig. 21 Final results

IV. CONCLUSION

The purpose of this paper was to make a comparative study of the behavior of the rim of a vehicle, made of four different materials, under the action of external loads. In order to determine the state of stresses and strains, 3D models of the rim were made using the Autodesk Inventor 2021 program and were analyzed by static analysis with the Nastran module.

The simulation shows that the maximum Von Mises voltage is low compared to the value of the flow limit regardless of the material chosen. Larger differences were obtained in terms of deformations, but these were in accordance with the mechanical properties of the materials. Following the comparative study for the four models, it can be specified that the importance of the material for the construction of the rims depends on the mass properties and their design.

The study can be continued with a more complex analysis of different types of rims and by studying the analysis of fatigue.

REFERENCES

[1] K. Venkateswara Rao and T. Dharmaraju, "Analysis of Wheel Rim Using Finite Element Method", International Journal of Engineering Research & Technology (IJERT), Vol. 3 Issue 1, ISSN: 2278-0181, January – 2014.

[2] J. Stearns, T. S. Srivatsan, X. Gao, and P. C. Lam, "Understanding the Influence of Pressure and Radial Loadson Stress and Displacement Response of a Rotating Body:The Automobile Wheel", Hindawi Publishing CorporationInternational Journal of Rotating Machinery, Article ID 60193, Pages1–8DOI 10.1155/IJRM/2006/60193, Volume 2006.

[3] B. Bimal, S. Adars, M. Akshay, K. Arun, J. Betson, R. Praveen, "Finite Element Analysis of Wheel Rim Using Abaqus Software", Int. Journal of Engineering Research and Application, ISSN : 2248-9622, Vol. 7, Issue 2, (Part -1), pp.31-34, February 2017.

[4] S. Kalpesh, P. Shailesh, "Design, FEM Analysis and of Alloy Wheel Rim of a Four Wheeler", International Advanced Research Journal in Science, Engineering and Technology ISO 3297:2007 Certified Vol. 4, Issue 9, ISSN (Online) 2393-8021 ISSN (Print) 2394-1588, September 2017.

[5] J. K. Rahul, S. G. Jadhav, "CAD Modeling and FEA Analysis of Wheel Rim for Weight Reduction", IJESC, Volume 6 Issue No. 6, DOI 10.4010/2016.1756, ISSN 2321 3361, 2016.

[6] T. B. Rakesh, B. Y. Tushar, Rewiew of Finite Element Analysis of Vehicle Rim", International Journal of Research in Engineering, Vol. No. 5, Special Issue No. (02), IJARSE, ISSN 2319-8354, March 2016.

[7] P. Meghashyam1, S. Girivardhan Naidu and N. Sayed Baba, "Design and Analysis of Wheel Rim using CATIA & ANSYS", International Journal of Application or Innovation in Engineering & Management (IJAIEM), Volume 2, Issue 8, August 2013.

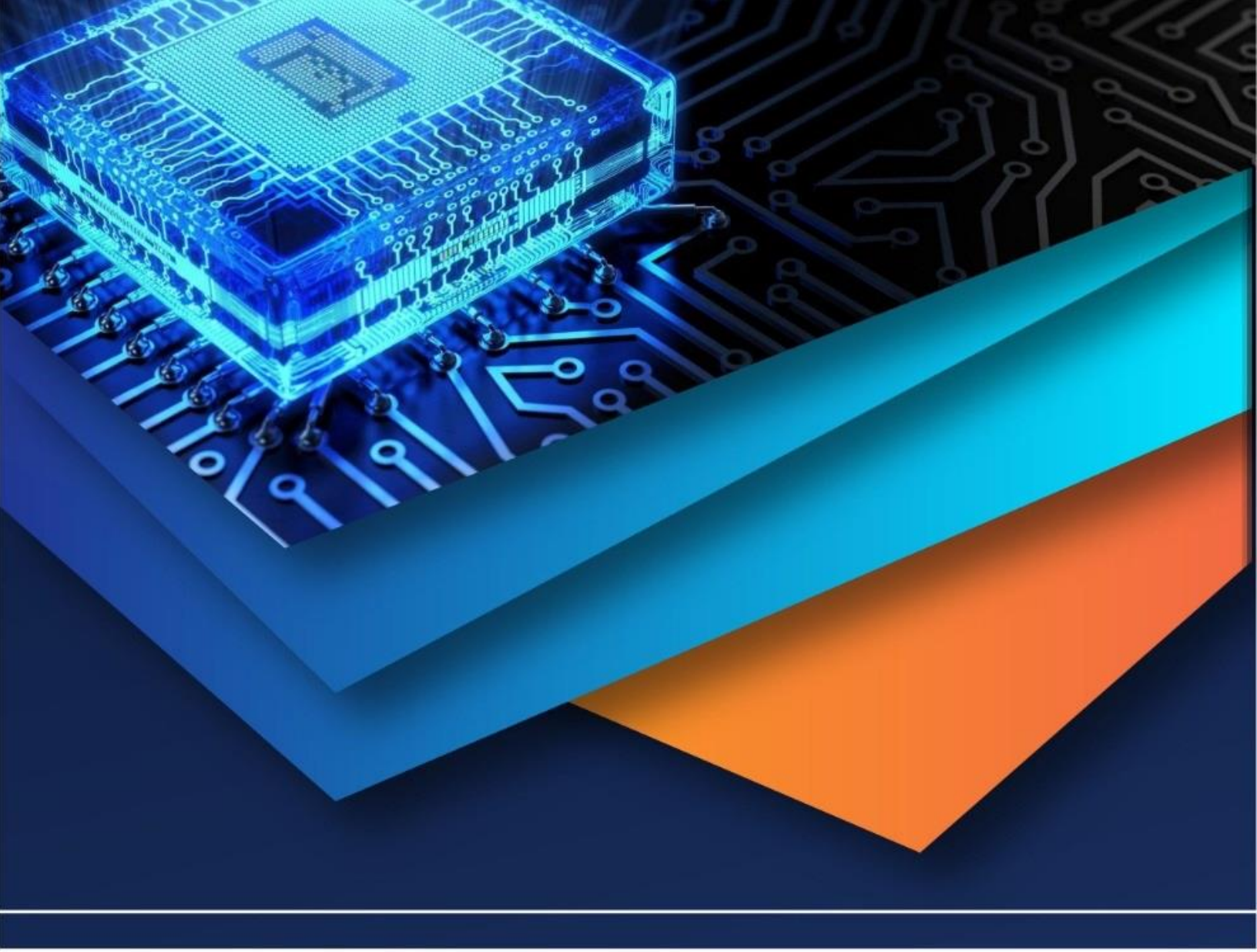

10.22214/IJRASET

45.98

IMPACT FACTOR: 7.129

IMPACT FACTOR: 7.429

INTERNATIONAL JOURNAL FOR RESEARCH

IN APPLIED SCIENCE & ENGINEERING TECHNOLOGY